Single-molecule fluorescence in redox chemistry

Jeuken, L.J.C.; Orrit, M.A.G.J.; Canters, G.W.

Available online at www.sciencedirect.com

ScienceDirect

Current Opinion in Electrochemistry

Review Article

Single-molecule fluorescence in redox chemistry

Lars Jeuken[1], Michel Orrit[2] and Gerard Canters[2]

Abstract

Optical studies of redox reactions are relatively non-invasive and can be performed in solution or on surfaces. These advantages are paired with advances in single-molecule and super-resolution methods. However, in electrochemistry, analysis is complicated by surface effects such as local heterogeneity in structure and chemistry, affecting redox thermodynamics and kinetics as well as the fluorescent properties of the dyes. We summarize single-molecule work done in our groups, in particular on single protein molecules, and discuss perspectives for future developments.

Addresses

[1] Leiden Institute of Chemistry, Gorlaeus Laboratory, Leiden University, Einsteinweg 55, 2333 CC, Leiden, the Netherlands

[2] Leiden Institute of Physics, Huygens-Kamerlingh Onnes Laboratory, Leiden University, Niels Bohrweg 2, 2333 CA, Leiden, the Netherlands

Corresponding author: Orrit, Michel (orrit@physics.leidenuniv.nl)

Current Opinion in Electrochemistry 2023, **37**:101196

This review comes from a themed issue on **Physical and Nanoelectrochemistry** (2023)

Edited by **Jeffrey E. Dick**

For a complete overview see the Issue and the Editorial

Available online 9 December 2022

https://doi.org/10.1016/j.coelec.2022.101196

Keywords

Single molecules, Fluorescence, Fluorogenic reactions, Redox reactions, Electrochemistry, Oxidation potential, Metallo-proteins, Azurin, Redox indicator, Methylene blue, Electron transfer, FRET, Labeled protein, Heterogeneity.

Introduction

The kinetics of most redox reactions are dependent on the dynamic interactions between two redox compounds or between an electrode and a redox compound. Grasping the complexity and the highly dynamical character of these interactions requires a full resolution of their heterogeneity in space and time. Steady progress in single-molecule experimentation has brought us nearer to the tantalizing goal of resolving electron transfer reactions in space and time. Processes such as diffusion, mobility and interactions of (macro)molecules, their chemical and mechanical reactivity and the influence of confinement, are mapped in ever increasing detail. Much information about redox reactions at the nanoscale has been provided by electrical and mechanical measurements with scanning probes and nanopores [1,2]. In this perspective, we focus on experiments done in far-field optical microscopy and spectroscopy [3–5]. They may be considered within the wider context of redox reactions. Single-molecule redox chemistry has been pursued using a variety of approaches and techniques, including electrochemistry, and after a brief introduction, we focus on some recent results obtained by fluorescence methods.

Single-molecule electrochemistry

A direct measurement of Faradaic electron transfer using electrochemistry is ultimately limited by the sensitivity of the amplifier or potentiostat. It has been estimated that quantification of electron transfer at the electrode surface is limited by electronic shot noise and requires the cumulative counting of at least 2000 electrons [6], prohibiting the electrochemical measurement of a single electron transfer step. A time resolution of 1 s for 2000 electrons limits the current sensitivity to 0.3 fA. Lemay and colleagues set an impressive benchmark in 2008 using lithography to fabricate sub-micron electrodes (100×100 nm^2). They measured an electrocatalytic proton reduction current of 22 fA by [NiFe]-hydrogenases using slow cyclic voltammetry (1.5 mV/s) [7]. Although hydrogenases are among the most active redox enzymes, with turnover rates of up to 9000 s^{-1}, the authors estimated that 22 fA still corresponds to the activity of 8–46 enzymes on the electrode. In other words, to measure single-molecule electrocatalysis, turnover rates well over 10,000 s^{-1} would be required, which are rarely encountered. Since publication of their report, several papers have reported single-molecule catalysis detected by nano-impact. In this approach, the adsorption of a catalyst on an electrode is monitored amperometrically, i.e., through the small current spikes caused by impact of individual catalyst particles. Vannoy et al. [8] reviewed several reports of such measurements and noted that in each case the observed catalytic turnover rates were several orders higher than found in ensemble measurements. They concluded that validation of these enhanced catalytic rates would require other independent methods.

The above detection limit only applies to direct measurements of an electrochemical current. If an intense

stream of particles can be influenced by single redox events, such events can be detected with much higher sensitivity, thanks to the inherent amplification provided by the intense particle stream. This idea can be applied with electrons in scanning tunnelling microscopes [9] and other nanojunctions [10], with field-effect transistors [11], with ions flowing through nanofluidic compartments [12] or nanopores [13], or with photons [14] reporting on the redox state of a suitable emitter. Here, we focus on this latter scheme applied through optical single-molecule signals. In applications of single-molecule optical microscopy to the study of redox reactions, we briefly describe the different solutions which have been shown to address two main experimental challenges: how to isolate single molecules experimentally and how to detect single redox events.

Experimental access to single molecules

How to isolate single molecules

To obtain optical access to single molecules experimentally, the illuminated detection volume must be limited, and a suitable optical signal must be isolated, usually through spectral resonance, from the background. In this article, we restrict ourselves to fluorescence, the most current optical technique in single-molecule optics. Single molecules can be spatially resolved in an optical microscope as soon as their density is so low that their point-spread functions do not overlap. Moreover, because acquisition times can be as long as minutes or hours, the molecules often are immobilized in the sample. Redox compounds can be immobilized directly on solid substrates possibly serving as electrodes, either through direct physisorption on a bare surface [15–17] or on self-assembled monolayers (SAMs) [18,19]. Alternatively, redox compounds can be immobilized in hydrogels [20], e.g., agarose [21], via covalent or transient tethers or linkers [22–27], on top of lipid bilayers on glass [28] or within liposomes [29–31]. Alternatively to immobilisation, Brownian motion can be actively compensated, by electrokinetic actuation [20,32] or by direct feedback on the sample stage [33]. Finally, molecules can be trapped in zero-mode wave guides [34], nanopores and nanochannels [35] or bipolar nanocells [36]. After isolating fluorescent emitters in space, their emission can be recorded by epi-fluorescent microscopy [29], TIRF [37] or confocal microscopy [24,38]. For the analysis of redox processes at long time scales, immobilisation on solid surfaces is often the most practical solution providing a fair balance between ease and experimental flexibility.

How to monitor the redox state through fluorescence

Distinguishing redox events of a single molecule requires identifying the transitions between two redox states. This requires the emission of many photons, of which, in customary experimental configurations, only a small fraction (usually, a few percent at best) are effectively detected. If the stream of detected photons changes according to the redox state of the object under study, one can identify change points in a time trace of intensity, spectrum, lifetime, or any other fluorescence observable. Such change points thus report on single redox turnover events. Monitoring changes in redox state requires many more photons than are needed for just detecting single molecules in the sample. Photostability of the fluorescent emitters is therefore an issue, unless the redox reaction itself is able to produce several fluorescent molecules in a so-called fluorogenic reaction, each of which may emit many photons before bleaching. With a fluorescence lifetime of 10 ns, a time resolution of 10 ms, and a detection quantum yield of 1%, a single molecule under continuous illumination generates up to 10^4 detected photons per data point, a signal strong enough for accurate recordings of redox time traces with single-channel photodetectors and cameras. As fluorescence can be observed against a nearly dark background, a difference in fluorescence intensity can be readily measured at the single-molecule level.

The challenge here, however, is to find a spectroscopic observable reporting on the redox state of the single molecule under study. Three classes of solutions have been proposed so far in single-molecule fluorescence studies, which are schematically illustrated in Figure 1. One typical case is illustrated in Figure 1a, in which one of the reactants of a reaction is coupled to a so-called fluorogenic reaction, upon which a fluorescent product is generated [39,40]. In this first scheme, for which we are not aware of any published example of single-molecule redox conversion, a catalyst or active site could switch between two redox states, one of which would be inactive and the other active, i.e., it would give rise to a stream of fluorescent products, themselves visualized by fluorescence. Thus fluorescence would report on the redox state of the catalyst. In a second class, a fluorescent species is one of the compounds involved in the redox reaction(s) (Figure 1b). In an early example, the redox state of a flavin co-factor (FAD) of cholesterol oxidase was monitored during turn-over, the fluorescence reporting on the redox state of flavin [41]. Another possibility is a change of the fluorescence properties of the reactant itself, for example the redox indicator methylene blue [38,42,43]. The third class of experiments involves a fluorescent label, attached in the vicinity of the reaction centre whose optical properties are affected by its redox state (Figure 1c) [19,20,24,26,44]. In that case, the label does not directly participate in the redox reaction, it merely reports on it by interacting with one of the reactants or products. A common interaction involves quenching of the label's fluorescence by energy transfer to one of the redox states, whereas quenching by the other state does not occur, or is significantly weaker. The latter approach is particularly attractive for redox proteins, because a wide variety of fluorescent dyes can be relatively easily conjugated to the proteins at *specific locations* without disrupting the overall properties of the

Figure 1

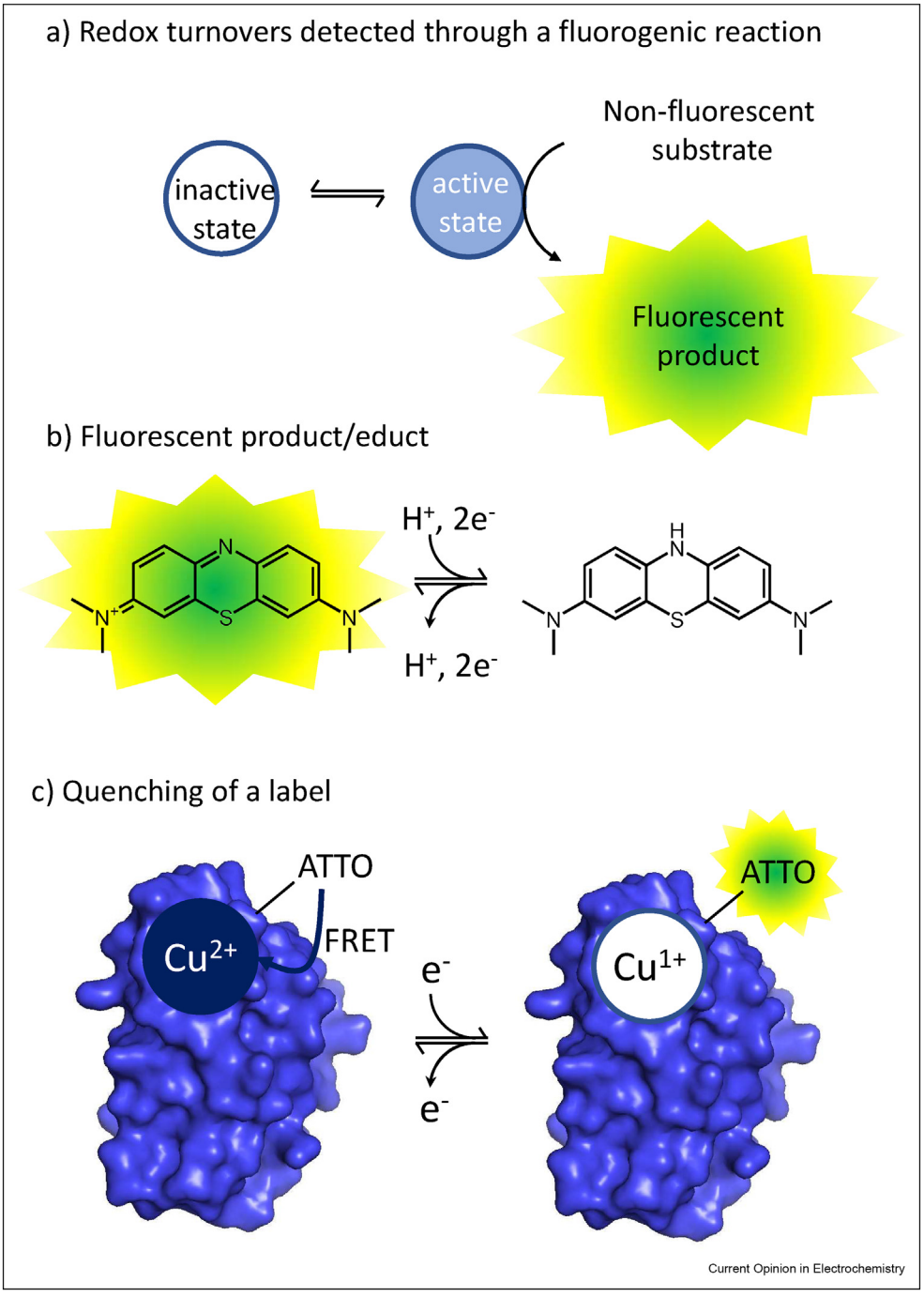

Three possible examples of fluorescence monitoring of a redox reaction. (**a**) The interconversion of an inactive state of a catalyst to a an active state is monitored by following the catalytic conversion of a non-fluorescent substrate to a fluorescent product. If the conversion of the inactive to the active catalyst would be due to a single redox reaction, these method could in principle be used to study a single electron transfer step. However, we are not aware of any example in which this method is used to study a single redox conversion of the catalyst. (**b**) One of the terms of the redox reaction, the educt or product, is fluorescent; (**c**) An auxiliary label is quenched by one of the terms of the redox reaction. (b) and (c) are illustrated in the text by methylene blue and labelled azurin, respectively.

redox sites. The particular case of azurin is discussed in detail in section Fluorescently labelled azurin. Table 1 presents a few examples of fluorescent systems reporting on various reactions, most of them of the redox type, and many of them at the single-molecule level.

In the following, two examples will be discussed in more detail. The first one deals with methylene blue, a dye whose fluorescence depends on its redox sate. Methylene blue fluorescence is very weak, but can be strongly enhanced by immobilizing the dye molecule in close proximity to a gold nanorod's tip, in its optical near field. The second example is presented by a non-fluorescent metalloprotein, azurin, whose redox state was monitored indirectly by conjugation to a fluorescent dye. These two examples can be considered as archetypes of the latter two classes of possible methods mentioned previously (Figure 1b and c).

Two case studies

Methylene blue

Methylene blue is a redox indicator, which changes from a strongly blue-coloured form in its oxidized state to the colourless leuco form in its reduced state. Although the change in absorption is spectacular in large ensembles of molecules, the absorption of a single methylene blue molecule is too weak to measure directly, and a fluorescence assay is needed. Unfortunately, the fluorescence yield of methylene blue is a few percent, which makes it difficult to detect the fluorescence of a single molecule, and even harder to measure fluorescence changes due to redox reactions. Following an earlier proposal to monitor the redox state of a fluorescent molecule [43], plasmonic enhancement of fluorescence was utilized in Ref. [42] to record redox time traces of single methylene blue molecules, which terminated when the dye photo-bleached. A relatively moderate fluorescence enhancement by the nearby tip of a single nanorod (by about 100 times) was achieved by immobilising methylene blue close to gold nanorods with a plasmon resonance overlapping significantly with its fluorescence spectrum. In this manner, long fluorescence time traces were recorded with sufficient signal-to-noise ratio to determine bright and dark times corresponding to oxidized and reduced states, respectively. Redox switching of methylene blue was monitored after reacting with an electron mediator, phenazine ethosulfate (PES), whose redox state in turn was controlled electrochemically using a nearby gold electrode. It was thus possible to determine the oxidation potential for a small number of single methylene blue molecules, and this potential was found to depend significantly on the particular molecule under study (Figure 2). Those variations were assigned to the particular microenvironment of each molecule and to the surrounding charge distribution, which affected the respective stabilities of the two redox forms. These experiments also demonstrated a small effect of the laser illumination on the redox properties of the fluorescent molecule. This influence was assigned to an increase in oxidation potential ($E^{0'}$) under optical excitation, resulting in an apparent rise in $E^{0'}$ under high excitation intensity.

The main weakness of this work was the very small number of molecules studied. Indeed, to ensure the single-molecule regime was reached, it was necessary to reduce the number of molecules per nanorod to much less than one on average, and it was very unlikely to find an isolated methylene blue molecule at the proper distance from a single gold nanorod. Hundreds of nanorods had to be identified and studied to determine whether a proper dye molecule was at the right distance and position. Consequently, once the dye molecule was bleached, the associated rod was lost for further studies. Future work on this or similar systems would benefit from transient binding of the redox molecule. Methylene blue molecules or other dyes would be conjugated, e.g., to single DNA oligomers, which could transiently hybridize to fixed complementary strands immobilized in the near field of the gold nanorod, as illustrated recently with a non-redox active near-infrared dye [23]. This scheme has the advantage that the dye can be renewed after bleaching, while the same active spot at a close distance from the gold nanorod is kept for further hybridization events.

Fluorescently labelled azurin

The second example relates to the non-fluorescent small blue copper protein azurin from *Pseudomonas aeruginosa* [22,24,44]. In its oxidized form, the copper site has a strong absorption band in the red giving the protein a beautiful blue appearance. When the protein is labelled with a fluorescent dye whose emission overlaps with the copper site's absorption, Förster resonance energy transfer (FRET) from the dye to the copper site will quench the dye fluorescence. In its reduced form, azurin is colourless and the dye now emits fluorescence unhindered. Hence, the fluorescence intensity or lifetime of an appropriately labelled azurin molecule directly reports on the oxidation state of its copper site. Under certain conditions, reversible electron transfer from the dye to the oxidized copper site can also occur [45]. Therefore, the distance between label and copper site should be chosen small enough for FRET, but large enough to prevent photo-induced electron transfer and the ensuing fluorescence quenching. This was achieved by labelling a Cy5 or ATTO647N to a unique cysteine engineered on the surface of azurin with site-directed mutagenesis (e.g., K27C or N42C). We have previously reported single-molecule measurements of azurin in solution by means of fluorescence correlation spectroscopy (FCS) [44]. Analysis of the redox state was performed by fluorescence intensity distribution analysis (FIDA),

Table 1

Examples of reactions that can (or could) provide a fluorescence readout of the redox state of single molecules.

Reaction detected	Dye/molecule name	ex/em (nm)	Reference	Comments
Oxidation and reduction of the fluorescent dye	Cresyl violet	598/621	[38,43]	Reducing the fluorescent dye Cresyl violet ($E^{0'} \approx -0.34$ V vs Ag/AgCl) creates a weakly-fluorescent compound
	Methylene blue (MB)	~665/~680	[42]	Oxidized MB is fluorescent, reduced leuco MB is non-fluorescent
	Resorufin	571/584	[51]	Reduction of the non-fluorescent resazurin results in the fluorescent resorufin
	Alexa Fluor 647	650/665	[37]	Proton-coupled reduction of Alexa Fluor 647 leads to a non-fluorescent product
Natural biological co-factors	NADH	~340/~460	[52]	NADH is fluorescent, but the oxidized NAD^+ is not
	Flavins	~370/~518 ~450/~518 (Riboflavin)	[41,52]	Oxidized flavin is fluorescent, reduced flavin is non-fluorescent (the hydroquinone is weakly fluorescent)
Oxidation of a quenching moiety	3′-(p-aminophenyl) fluorescein (APF)	492/514	[53]	Fluorescein is quenched by a p-aminophenyl. Illumination induces a one-electron oxidation of the p-aminophenyl group, restoring fluorescence.
	H_2B-PMHC (BODIPY)	500/530	[54]	BODIPY is quenched by a topopherol group. Oxidation of the topopherol-quenching group restores BODIPY fluorescence
Measuring products of redox reactions	Fluorescein	480/515	[55]	Electrochemical reduction of water is measured by pH changes, changing fluorescence intensity of the pH-sensitive dye, fluorescein.
Non-redox fluorogenic reaction	N-(1-nonyldecyl)-N′-(p-aminophenyl) perylene 3,4,9,10-tetracarboxyl bisimide (NDAPP)	~522/~533	[56]	The fluorescent dye (perylene) is quenched by a p-aminophenyl group. Upon protonation (or metal binding) of the quenching group, fluorescence is restored.
	Molecular ‘beacon’ with fluorophore FITC and quencher DABCYL	490/520	[57]	The fluorophore and quencher are connected via a short peptide. Fluorescence is restored upon cleavage of the peptide linker.
	Bridged Carboxy-Fluorescein BCECF-AM	490/520	[39]	A chemically modified form of the fluorescent dye BCECF. After enzymatic conversion, BCECF and its fluorescence are restored.

Figure 2

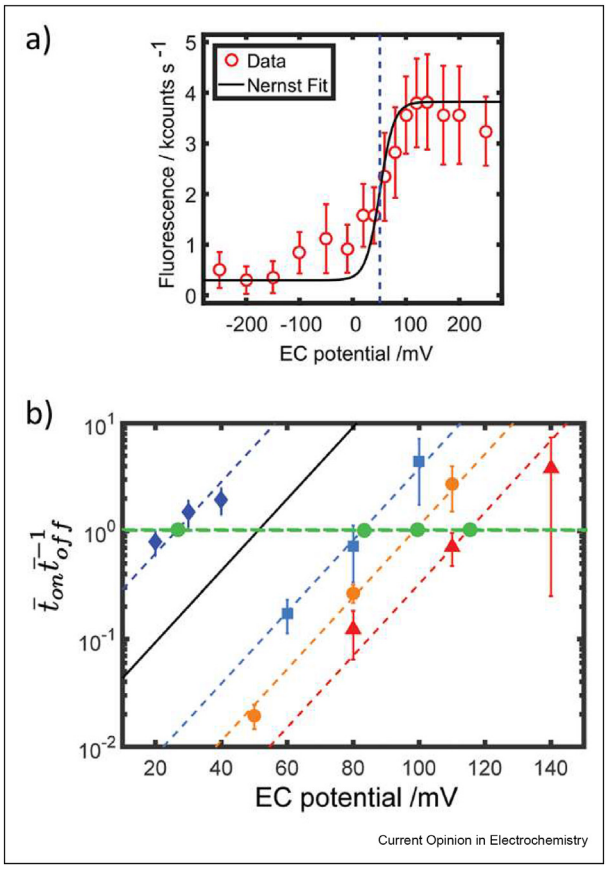

a) Ensemble fluorescence response of 260 unenhanced methylene blue molecules to the electrochemical potential, showing the controlled switching from the reduced state at low potentials to the oxidized state at high potentials. The black curve is a fit using the Nernst equation and the dashed line illustrates the obtained oxidation potential (51 ± 4 mV). **b**) The ratio of the average lifetimes in the oxidized ($\overline{t_{on}}$) and reduced ($\overline{t_{off}}$) state of the methylene blue ($\overline{t_{on}}/\overline{t_{off}}$) is plotted as a function of the potential for four single, surface-immobilised methylene blue molecules for which the fluorescence is plasmonically enhanced using nearby gold nanorods. The EC potential is set by the electron mediator phenazine ethosulphate (PES), whose redox potential is controlled electrochemically *via* nearby gold electrodes. Different symbols and colours represent different single molecules. The diagonal dashed lines are fits of these data using the Nernst equation to extract the oxidation potential E_0 for each molecule, while the black solid line corresponds to the ensemble value of the oxidation potential extracted from data in Figure a). The green dashed line represents $\overline{t_{on}} = \overline{t_{off}}$, when methylene blue spends half its time oxidised and the other half reduced. This half-wave potential thus equals the oxidation potential, $E^{0'}$, of the four single methylene blue molecules under study (indicated by green dots). Figure based on Figures 2b and 4b of ref. [42], reproduced with permission.

which reports on the redox state of the copper site in azurin. Although they could distinguish oxidised and reduced azurin states, FCS and FIDA provided little data on the actual redox switching. In order to monitor changes in redox state of single molecules, it was thus necessary to isolate the redox compounds for extended periods of time, by confining the fluorescent molecules in a small volume or by sparsely immobilizing them on an electrode surface.

In redox studies of single proteins, the dye-protein couple and the attachment site have to be considered carefully. In early experiments with Cy5-azurin, the molecules were immobilized on a glass cover slip and oxidised and reduced with chemical agents [22,44]. Fluorescence was significantly quenched in the oxidised Cy5-azurin and not in the reduced Cy5-azurin and thus reversible oxidation and reduction of single azurins could be monitored with fluorescence microscopy, until the Cy5 dye photobleached [44]. Unexpectedly, however, Cy5-(K27C)-azurin displayed two species with different fluorescence intensities, both in their oxidised and reduced states. Similarly, two species were observed for the redox inactive and colourless Zn-azurin, in which the copper ion is replaced by a zinc. As these two species were not observed for the free dye, the two intensities were attributed to two specific conformations of the Cy5 label at the K27C position of azurin, independent of its redox state. Conformational flexibility of the dye at the protein surface should thus be considered when choosing an appropriate conjugation site and dye. Later, Cy5-azurin was immobilized on the working electrode of a three-electrode electrochemical cell and monitored optically. The redox state of azurin was changed by direct electron exchange with a gold electrode coated with a SAM of alkanethiol, which for a proper alkane length (less than 10 carbons) enables electrochemical oxidation and reduction of immobilized azurin [46]. Ensemble experiments showed a good correspondence between the electrochemical and fluorescence signals [19], taking into account quenching of the Cy5 by gold [24].

More recent studies on ATTO647N−N42C-azurin (and of an ATTO655-Azurin variant) made sure that only a single fluorescent species is observed in the oxidised state [22]. This enabled a fluorescence study of ATTO647N−N42C-azurin tethered to glass *via* a long (20 nm) linker, whereas redox switching was controlled by ferri/ferrocyanide in solution (Figure 3). The redox couple ferri/ferrocyanide was controlled electrochemically via a Pt electrode positioned close to the glass surface. A continuous range of potentials was applied, effectively providing a potentiometric titration monitored at the single-protein level. Detailed analysis of 145 individual ATTO647N−N42C-azurin molecules indicated a distribution in reduction potentials. The reduction potentials followed a Gaussian-like distribution with a FWHM of 45 mV. Importantly, the distribution of oxidation potentials is significantly narrower than found in previous analysis of fluorescently labelled azurins adsorbed on alkanethiol SAMs [19,47] suggesting that flexibility of the 20-nm long tether averaged out local surface charge inhomogeneities to a large extent. Yet,

Figure 3

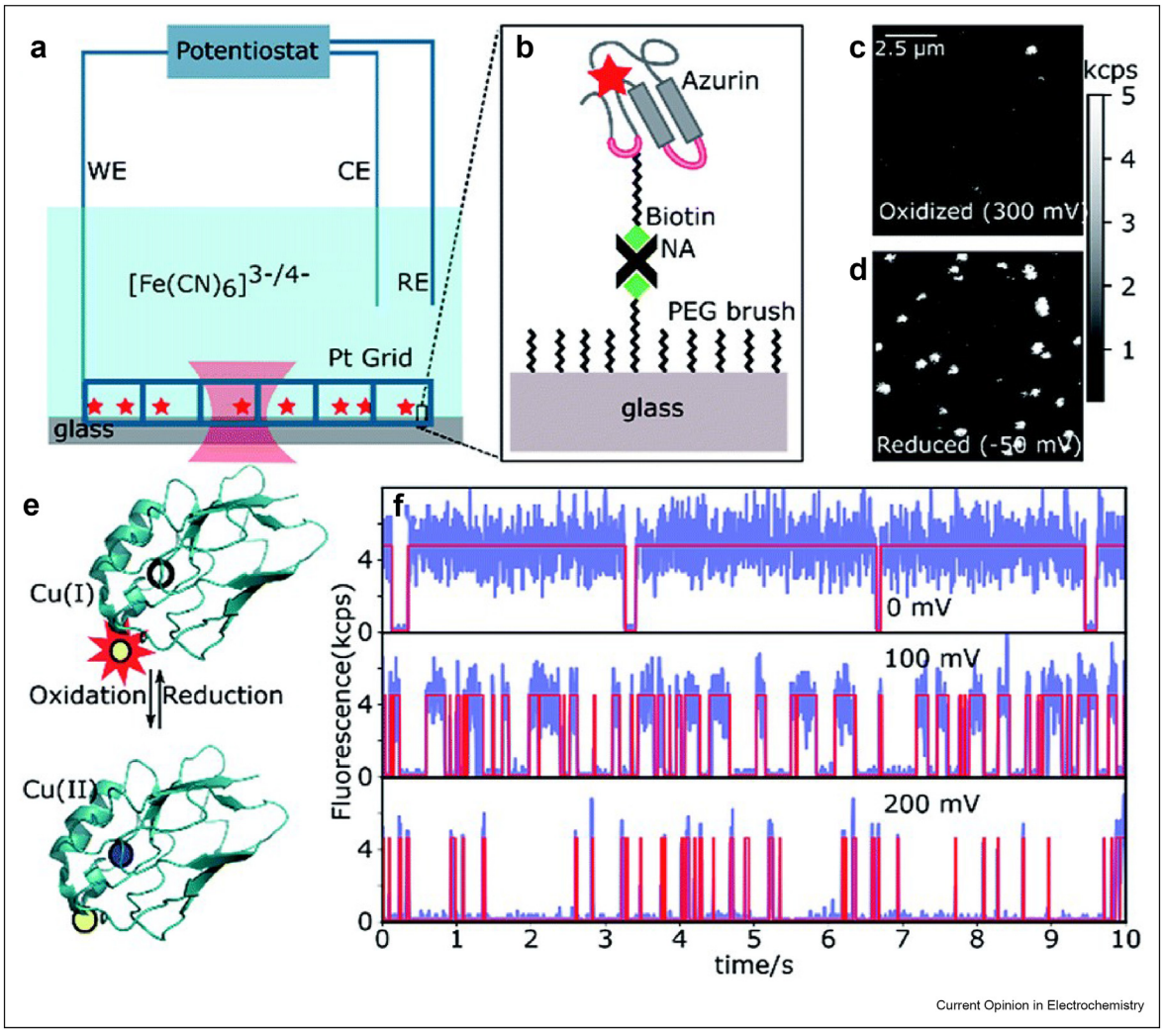

Single azurin imaging and intensity traces at different potentials. (**a**) Scheme of the electrochemical system with confocal laser spot (red waist). The electrochemical setup consists of a potentiostat, a platinum grid as working electrode (WE), a platinum coil as counter electrode (CE), and an SCE as the reference electrode (RE). (**b**) Schematic of the immobilization of azurin on a PEG-passivated glass surface through NeutrAvidin–biotin binding. (**c** and **d**) Confocal images of the same area of a functionalized glass slide at oxidizing (C, 300 mV) and reducing (D, –50 mV) potential, respectively. (**e**) Azurin structure with reduced Cu (top, empty dot) and oxidized Cu (bottom, blue dot) and the dye (yellow) in the associated state (bright, symbolized by the red star, at the top quenched at the bottom). (**f**) Three time traces of the same single azurin molecule at 0 mV, 100 mV and 200 mV (binning time 5 ms). Note the variations in the average durations of bright and dark times at different potentials. Figure reproduced from Ref. [22] with permission from the Royal Society of Chemistry.

this dispersion of oxidation potentials was still well beyond that expected for statistical error. Further analysis of 13 molecules of ATTO647N–N42C-azurin over time periods up to thousands of seconds further demonstrated dynamic heterogeneity of reduced and oxidised dwell times. This heterogeneity appears as correlated successions of (bright or dark) times longer or shorter than their average. Dynamical heterogeneity, which has been observed earlier in single-enzyme kinetics [39,48], is assigned to multiple conformational states of the same single molecule, which may not only influence the reaction rates, but potentially also the oxidation potential of the single molecule. Long-lived structural heterogeneity may also cause variations in association rates between the ferri/ferrocyanide and azurin.

Perspectives

The last decade has seen the first experiments combining redox chemistry with single molecules, typically immobilized on a surface. But what can we expect from these single-molecule experiments?

Because of the complexity and heterogeneity of surfaces, electron transfer processes and redox properties of individual (macro)molecules are subject to heterogeneity in space and time, meaning that reaction parameters such as oxidation potentials, potential barriers, reorganization energies, etc. will fluctuate from molecule to molecule and will also fluctuate as a function of time for the same single molecule. Studying these distributions, we can hope for a better understanding and control of these reactions.

Moreover, because they do not need synchronization of many individual molecules, experiments on a single molecule can reveal mechanistic details that are hidden in ensemble-averaged experiments, such as the sequences of intermediate states occupied in a complex reaction, or predecessor-successor relations between these states, or the potential energy landscape with favoured reaction pathways.

The main access to the redox states of a molecule so far has been fluorescence. A first access applied earlier in catalysis makes use of fluorogenic reactions, which, e. g., produce a fluorescent molecule from a non-fluorescent reactant. The intensity of fluorescence therefore reports on the activity of the reactive site. A more direct method, illustrated here with methylene blue, detects the redox state of the molecule of interest through its fluorescence directly. When one of the redox states absorbs differently from the other, but is not fluorescent, quenching of a nearby fluorescent dye can be used to detect redox reactions. This process has been illustrated here by the case of azurin, but could be extended to multicentre enzymes, for example those involved in mitochondrial or photosynthetic respiratory cycles. Different redox sites could be labelled by specific dyes to follow the different reactions and their interactions.

Finally, optical single-molecule methods are no longer limited to fluorescence. Scattering experiments either in bright field (iSCAT) [49] or by photothermal contrast [50], could be adapted to redox reactions if the absorption or polarizability of the molecule or nanoparticle under study changes under the influence of the reaction. In view of our urgent need for efficient energy conversion and thus for better understanding and control of electrochemical reactions, we can expect much more single-entity experiments and applications in the future.

Declaration of competing interest

The authors declare that they have no known competing financial interests or personal relationships that could have appeared to influence the work reported in this paper.

Data availability

No data was used for the research described in the article.

Acknowledgements

The experiments discussed here succeeded thanks to the hard work of many PhD students and postdoctoral fellows over many years. We are particularly grateful to Drs. Weichun Zhang, Biswajit Pradhan, and Martín Caldarola. We thank Dr. Claudio Saracini, Naples, for stimulating discussions on the subject of multicentre respiratory enzymes. Continuing financial support by NWO is gratefully acknowledged.

References

Papers of particular interest, published within the period of review, have been highlighted as:

- • of special interest
- •• of outstanding interest

1. Fu KY, Kwon SR, Han D, Bohn PW: **Single entity electrochemistry in nanopore electrode arrays: ion transport meets electron transfer in confined geometries**. *Acc Chem Res* 2020, **53**:719–728, https://doi.org/10.1021/acs.accounts.9b00543.

2. Oja SM, Fan YS, Armstrong CM, Defnet P, Zhang B: **Nanoscale electrochemistry revisited**. *Anal Chem* 2016, **88**:414–430, https://doi.org/10.1021/acs.analchem.5b04542.

3. Akkilic N, Geschwindner S, Hook F: **Single-molecule biosensors: recent advances and applications**. *Biosens Bioelectron* 2020, **151**, 111944, https://doi.org/10.1016/j.bios.2019.111944.

4. Hao R, Peng ZY, Zhang B: **Single-molecule fluorescence microscopy for probing the electrochemical interface**. *ACS Omega* 2020, **5**:89–97, https://doi.org/10.1021/acsomega.9b03763.

5. Wang W: **Imaging the chemical activity of single nanoparticles with optical microscopy**. *Chem Soc Rev* 2018, **47**:2485–2508, https://doi.org/10.1039/c7cs00451f.

6. Gao R, Edwards MA, Harris JM, White HS: **Shot noise sets the limit of quantification in electrochemical measurements**. *Curr Opin Electroche* 2020, **22**:170–177, https://doi.org/10.1016/j.coelec.2020.05.010.

7. •• Hoeben FJM, Meijer FS, Dekker C, Albracht SPJ, Heering HA, Lemay SG: **Toward single-enzyme molecule electrochemistry: [nife]-hydrogenase protein film voltammetry at nanoelectrodes**. *ACS Nano* 2008, **2**:2497–2504, https://doi.org/10.1021/nn800518d.

This manuscript set a yet unbroken benchmark for trying to minimize the area of electrodes for single-enzyme electrochemistry. Although, ultimately single-enzyme conditions were not met, it clearly highlights the possibilities and limitations of reducing electrode area for single-enzyme electrochemistry.

8. Vannoy KJ, Ryabykh A, Chapoval AI, Dick JE: **Single enzyme electroanalysis**. *Analyst* 2021, **146**:3413–3421, https://doi.org/10.1039/d1an00230a.

9. Doppagne B, Chong MC, Bulou H, Boeglin A, Scheurer F, Schull G: **Electrofluorochromism at the single-molecule level**. *Science* 2018, **361**:251–254, https://doi.org/10.1126/science.aat1603.

10. Evers F, Korytar R, Tewari S, van Ruitenbeek JM: **Advances and challenges in single-molecule electron transport**. *Rev Mod Phys* 2020, **92**, 035001, https://doi.org/10.1103/RevModPhys.92.035001.

11. Gao N, Zhou W, Jiang XC, Hong GS, Fu TM, Lieber CM: **General strategy for biodetection in high ionic strength solutions using transistor-based nanoelectronic sensors**. *Nano Lett* 2015, **15**:2143–2148, https://doi.org/10.1021/acs.nanolett.5b00133.

12. Kostiuchenko ZA, Lemay SG: **Quasi-one-dimensional generator-collector electrochemistry in nanochannels**. *Anal Chem* 2020, **92**:2847–2852, https://doi.org/10.1021/acs.analchem.9b05396.

13. Brinkerhoff H, Kang ASW, Liu JQ, Aksimentiev A, Dekker C: **Multiple rereads of single proteins at single-amino acid resolution using nanopores**. *Science* 2021, **374**:1509–1513, https://doi.org/10.1126/science.abl4381.

14. Mathwig K, Aartsma TJ, Canters GW, Lemay SG: **Nanoscale methods for single-molecule electrochemistry**. *Annu Rev Anal Chem* 2014, **7**:383–404, https://doi.org/10.1146/annurev-anchem-062012-092557.

15. Bizzotto D: **In situ spectroelectrochemical fluorescence microscopy for studying electrodes modified by molecular adsorbates**. *Curr Opin Electroche* 2018, **7**:161–171, https://doi.org/10.1016/j.coelec.2017.11.019.

16. Davis JJ, Halliwell CM, Hill HAO, Canters GW, van Amsterdam MC, Verbeet MP: **Protein adsorption at a gold electrode studied by in situ scanning tunnelling microscopy**. *New J Chem* 1998, **22**:1119–1123, https://doi.org/10.1039/a803384f.

17. Chi QJ, Zhang JD, Nielsen JU, Friis EP, Chorkendorff I, Canters GW, Andersen JET, Ulstrup J: **Molecular monolayers and interfacial electron transfer of pseudomonas aeruginosa azurin on Au(111)**. *J Am Chem Soc* 2000, **122**:4047–4055, https://doi.org/10.1021/ja993174t.

18. Krzeminski L, Ndamba L, Canters GW, Aartsma TJ, Evans SD, Jeuken LJC: **Spectroelectrochemical investigation of intramolecular and interfacial electron-transfer rates reveals differences between nitrite reductase at rest and during turnover**. *J Am Chem Soc* 2011, **133**:15085–15093, https://doi.org/10.1021/Ja204891v.

19. Salverda JM, Patil AV, Mizzon G, Kuznetsova S, Zauner G, Akkilic N, Canters GW, Davis JJ, Heering HA, Aartsma TJ: **Fluorescent cyclic voltammetry of immobilized azurin: direct observation of thermodynamic and kinetic heterogeneity**. *Angew Chem Int Ed* 2010, **49**:5776–5779, https://doi.org/10.1002/anie.201001298.

20. •• Goldsmith RH, Tabares LC, Kostrz D, Dennison C, Aartsma TJ, Canters GW, Moerner WE: **Redox cycling and kinetic analysis of single molecules of solution-phase nitrite reductase**. *Proc Nat Acad Sci USA* 2011, **108**:17269–17274, https://doi.org/10.1073/pnas.1113572108.

Confinement of single molecules of blue nitrite reductase in an electrokinetic anti-Brownian trap allows the observation of individual redox events not perturbed by contact with surfaces. Microscopic kinetic parameters are extracted compatible with a random sequential enzyme mechanism. It is the first report on single enzyme molecules operating free in solution.

21. Tabares LC, Kostrz D, Elmalk A, Andreoni A, Dennison C, Aartsma TJ, Canters GW: **Fluorescence lifetime analysis of nitrite reductase from alcaligenes xylosoxidans at the single-molecule level reveals the enzyme mechanism**. *Chem Eur J* 2011, **17**:12015–12019, https://doi.org/10.1002/chem.201102063.

22. •• Pradhan B, Engelhard C, Van Mulken S, Miao XY, Canters GW, Orrit M: **Single electron transfer events and dynamical heterogeneity in the small protein azurin from pseudomonas aeruginosa**. *Chem Sci* 2020, **11**:763–771, https://doi.org/10.1039/c9sc05405g.

The fluorescence of single-dye-labeled-molecules of the small blue copper protein azurin undergoing electron transfer (ET) reactions with hexacyanoferrate was monitored under controlled electrochemical potential. Dynamical heterogeneity was held responsible for the observed significant fluctuations in ET rates and midpoint potentials following a 'punctuated equilibrium' model. The fluctations could be tied in a unique and quantitative way to variations in molecular parameters (driving force, D-A coupling, complex association constants or structural variations).

23. Zhang WC, Caldarola M, Lu XX, Pradhan B, Orrit M: **Single-molecule fluorescence enhancement of a near-infrared dye by gold nanorods using DNA transient binding**. *Phys Chem Chem Phys* 2018, **20**:20468–20475, https://doi.org/10.1039/c8cp03114b.

24. Elmalk AT, Salverda JM, Tabares LC, Canters GW, Aartsma TJ: **Probing redox proteins on a gold surface by single molecule fluorescence spectroscopy**. *J Chem Phys* 2012, **136**, 235101, https://doi.org/10.1063/1.4728107.

25. Rinaldi R, Biasco A, Maruccio G, Arima V, Visconti P, Cingolani R, Facci P, De Rienzo F, Di Felice R, Molinari E, *et al.*: **Electronic rectification in protein devices**. *Appl Phys Lett* 2003, **82**:472–474, https://doi.org/10.1063/1.1530748.

26. Kuznetsova S, Zauner G, Aartsma TJ, Engelkamp H, Hatzakis N, Rowan AE, Nolte RJM, Christianen PCM, Canters GW: **The enzyme mechanism of nitrite reductase studied at single-molecule level**. *Proc Nat Acad Sci USA* 2008, **105**:3250–3255, https://doi.org/10.1073/pnas.0707736105.

27. Jungmann R, Steinhauer C, Scheible M, Kuzyk A, Tinnefeld P, Simmel FC: **Single-molecule kinetics and super-resolution microscopy by fluorescence imaging of transient binding on DNA origami**. *Nano Lett* 2010, **10**:4756–4761, https://doi.org/10.1021/nl103427w.

28. Pradhan B, Khatua S, Gupta A, Aartsma T, Canters G, Orrit M: **Gold-nanorod-enhanced fluorescence correlation spectroscopy of fluorophores with high quantum yield in lipid bilayers**. *J Phys Chem C* 2016, **120**:25996–26003, https://doi.org/10.1021/acs.jpcc.6b07875.

29. Li M, Jorgensen SK, McMillan DGG, Krzemniski L, Daskalakis NN, Partanen RH, Tutkus M, Tuma R, Stamou D, Hatzakis NS, *et al.*: **Single enzyme experiments reveal a long-lifetime proton leak state in a heme-copper oxidase**. *J Am Chem Soc* 2015, **137**:16055–16063, https://doi.org/10.1021/jacs.5b08798.

30. Li MQ, Khan S, Rong HL, Tuma R, Hatzakis NS, Jeuken LJC: **Effects of membrane curvature and pH on proton pumping activity of single cytochrome bo(3) enzymes**. *Biochem Biophys Acta - Bioenerg* 2017, **1858**:763–770, https://doi.org/10.1016/j.bbabio.2017.06.003.

31. Boukobza E, Sonnenfeld A, Haran G: **Immobilization in surface-tethered lipid vesicles as a new tool for single biomolecule spectroscopy**. *J Phys Chem B* 2001, **105**:12165–12170, https://doi.org/10.1021/jp012016x.

32. Cohen AE, Moerner WE: **Suppressing brownian motion of individual biomolecules in solution**. *Proc Nat Acad Sci USA* 2006, **103**:4362–4365, https://doi.org/10.1073/pnas.0509976103.

33. Welsher K, Yang H: **Multi-resolution 3d visualization of the early stages of cellular uptake of peptide-coated nanoparticles**. *Nat Nanotechnol* 2014, **9**:198–203, https://doi.org/10.1038/Nnano.2014.12.

34. Zhao J, Zaino LP, Bohn PW: **Potential-dependent single molecule blinking dynamics for flavin adenine dinucleotide covalently immobilized in zero-mode waveguide array of working electrodes**. *Faraday Discuss* 2013, **164**:57–69, https://doi.org/10.1039/c3fd00013c.

35. Lu J, Fan Y, Howard MD, Vaughan JC, Zhang B: **Single-molecule electrochemistry on a porous silica-coated electrode**. *J Am Chem Soc* 2017, **139**:2964–2971, https://doi.org/10.1021/jacs.6b10191.

36. Fan Y, Hao R, Han C, Zhang B: **Counting single redox molecules in a nanoscale electrochemical cell**. *Anal Chem* 2018, **90**:13837–13841, https://doi.org/10.1021/acs.analchem.8b04659.

37. Fan S, Webb JEA, Yang Y, Nieves DJ, Gonçales VR, Tran J, Hilzenrat G, Kahram M, Tilley RD, Gaus K, *et al.*: **Observing the reversible single molecule electrochemistry of alexa fluor 647 dyes by total internal reflection fluorescence microscopy**. *Angew Chem Int Ed* 2019, **58**:14495–14498, https://doi.org/10.1002/anie.201907298.

38. • Lei CH, Hu DH: **High throughput mapping of single molecules' redox potentials on electrode**. *Anal Chem* 2021, **93**:8864–8871, https://doi.org/10.1021/acs.analchem.1c00984.

This work addresses the problem that fluctuations in fluorescence intensity can both be due to photodriven process and due to redox events under study. A high-throughput method is presented in which cross-correlation of fluctuations is able to distinguish between both processes.

39. • Velonia K, Flomenbom O, Loos D, Masuo S, Cotlet M, Engelborghs Y, Hofkens J, Rowan AE, Klafter J, Nolte RJM, *et al.*: **Single-enzyme kinetics of calb-catalyzed hydrolysis**. *Angew Chem Int Ed* 2005, **44**:560–564, https://doi.org/10.1002/anie.200460625.

Evidence for the dynamical heterogeneity of a lipase enzyme in single-molecule time traces.

40. Zhou XC, Xu WL, Liu GK, Panda D, Chen P: **Size-dependent catalytic activity and dynamics of gold nanoparticles at the single-molecule level**. *J Am Chem Soc* 2010, **132**:138–146, https://doi.org/10.1021/ja904307n.

41. • Lu HP, Xun LY, Xie XS: **Single-molecule enzymatic dynamics**. *Science* 1998, **282**:1877–1882, https://doi.org/10.1126/science.282.5395.1877.
First long time traces of single enzymes. Evidence for dynamical heterogeneity due to conformational dynamics of the enzyme.

42. •• Zhang WC, Caldarola M, Pradhan B, Orrit M: **Gold nanorod enhanced fluorescence enables single-molecule electrochemistry of methylene blue**. *Angew Chem Int Ed* 2017, **56**:3566–3569, https://doi.org/10.1002/anie.201612389.
Discussion of single-molecule fluorescence time traces of a redox indicator, methylene blue, displaying dark and bright times corresponding to reduced and oxidized traces of the dye. The oxidation potential is found to vary from molecule to molecule

43. Lei CH, Hu DH, Ackerman EJ: **Single-molecule fluorescence spectroelectrochemistry of cresyl violet**. *Chem Commun* 2008:5490–5492, https://doi.org/10.1039/b812161c.

44. Schmauder R, Librizzi F, Canters GW, Schmidt T, Aartsma TJ: **The oxidation state of a protein observed molecule-by-molecule**. *ChemPhysChem* 2005, **6**:1381–1386, https://doi.org/10.1002/cphc.200400628.

45. Andreoni A, Sen S, Hagedoorn PL, Buma WJ, Aartsma TJ, Canters GW: **Fluorescence correlation spectroscopy of labeled azurin reveals photoinduced electron transfer between label and Cu center**. *Chem Eur J* 2018, **24**:646–654, https://doi.org/10.1002/chem.201703733.

46. Murgida DH: **In situ spectroelectrochemical investigations of electrode-confined electron-transferring proteins and redox enzymes**. *ACS Omega* 2021, **6**:3435–3446, https://doi.org/10.1021/acsomega.0c05746.

47. Patil AV, Davis JJ: **Visualizing and tuning thermodynamic dispersion in metalloprotein monolayers**. *J Am Chem Soc* 2010, **132**:16938–16944, https://doi.org/10.1021/ja1065448.

48. • Yang H, Luo GB, Karnchanaphanurach P, Louie TM, Rech I, Cova S, Xun LY, Xie XS: **Protein conformational dynamics probed by single-molecule electron transfer**. *Science* 2003, **302**:262–266, https://doi.org/10.1126/science.1086911.
Single-enzyme study showing dynamical heterogeneity and the sensitivity of fluorescence to quenching that is mediated through photo-induced intramolecular electron-transfer processes.

49. Ortega-Arroyo J, Kukura P: **Interferometric scattering microscopy (iscat): new frontiers in ultrafast and ultrasensitive optical microscopy**. *Phys Chem Chem Phys* 2012, **14**:15625–15636, https://doi.org/10.1039/c2cp41013c.

50. Zijlstra P, Paulo PMR, Orrit M: **Optical detection of single non-absorbing molecules using the surface plasmon resonance of a gold nanorod**. *Nat Nanotechnol* 2012, **7**:379–382, https://doi.org/10.1038/Nnano.2012.51.

51. Andoy NM, Zhou X, Choudhary E, Shen H, Liu G, Chen P: **Single-molecule catalysis mapping quantifies site-specific activity and uncovers radial activity gradient on single 2d nanocrystals**. *J Am Chem Soc* 2013, **135**:1845–1852, https://doi.org/10.1021/ja309948y.

52. Chowdhury MH, Lakowicz JR, Ray K: **Ensemble and single molecule studies on the use of metallic nanostructures to enhance the intrinsic emission of enzyme cofactors**. *J Phys Chem C* 2011, **115**:7298–7308, https://doi.org/10.1021/jp112255j.

53. Tachikawa T, Yamashita S, Majima T: **Probing photocatalytic active sites on a single titanosilicate zeolite with a redox-responsive fluorescent dye**. *Angew Chem Int Ed* 2010, **49**:432–435, https://doi.org/10.1002/anie.200904876.

54. Godin R, Cosa G: **Counting single redox turnovers: fluorogenic antioxidant conversion and mass transport visualization via single molecule spectroelectrochemistry**. *J Phys Chem C* 2016, **120**:15349–15353, https://doi.org/10.1021/acs.jpcc.6b06183.

55. Engstrom RC, Ghaffari S, Qu H: **Fluorescence imaging of electrode-solution interfacial processes**. *Anal Chem* 1992, **64**:2525–2529, https://doi.org/10.1021/ac00045a012.

56. Zang L, Liu R, Holman MW, Nguyen KT, Adams DM: **A single-molecule probe based on intramolecular electron transfer**. *J Am Chem Soc* 2002, **124**:10640–10641, https://doi.org/10.1021/ja0268074.

57. Yu Z, Zhou L, Zhang T, Shen R, Li C, Fang X, Griffiths G, Liu J: **Sensitive detection of mmp9 enzymatic activities in single cell-encapsulated microdroplets as an assay of cancer cell invasiveness**. *ACS Sens* 2017, **2**:626–634, https://doi.org/10.1021/acssensors.6b00731.